An Integrated Fluorescence Detection System in Poly(dimethylsiloxane) for Microfluidic Applications

Michael L. Chabinyc, Daniel T. Chiu, J. Cooper McDonald, Abraham D. Stroock, James F. Christian, Arieh M. Karger, and George M. Whitesides

Department of Chemistry and Chemical Biology, Harvard University, 12 Oxford Street, Cambridge, Massachusetts 02138, and Radiation Monitoring Devices, Inc., Watertown, Massachusetts 02472

ANALYTICAL® CHEMISTRY

Reprinted from
Volume 73, Number 18, Pages 4491–4498

Anal. Chem. **2001**, *73*, 4491−4498

An Integrated Fluorescence Detection System in Poly(dimethylsiloxane) for Microfluidic Applications

Michael L. Chabinyc,† Daniel T. Chiu,† J. Cooper McDonald,† Abraham D. Stroock,† James F. Christian,‡ Arieh M. Karger,‡ and George M. Whitesides*,†

Department of Chemistry and Chemical Biology, Harvard University, 12 Oxford Street, Cambridge, Massachusetts 02138, and Radiation Monitoring Devices, Inc., Watertown, Massachusetts 02472

This paper describes a prototype of an integrated fluorescence detection system that uses a microavalanche photodiode (μAPD) as the photodetector for microfluidic devices fabricated in poly(dimethylsiloxane) (PDMS). The prototype device consisted of a reusable detection system and a disposable microfluidic system that was fabricated using rapid prototyping. The first step of the procedure was the fabrication of microfluidic channels in PDMS and the encapsulation of a multimode optical fiber (100-μm core diameter) in the PDMS; the tip of the fiber was placed next to the side wall of one of the channels. The optical fiber was used to couple light into the microchannel for the excitation of fluorescent analytes. The photodetector, a prototype solid-state μAPD array, was embedded in a thick slab (1 cm) of PDMS. A thin (80 μm) colored polycarbonate filter was placed on the top of the embedded μAPD to absorb scattered excitation light before it reached the detector. The μAPD was placed below the microchannel and orthogonal to the axis of the optical fiber. The close proximity (~200 μm) of the μAPD to the microchannel made it unnecessary to incorporate transfer optics; the pixel size of the μAPD (30 μm) matched the dimensions of the channels (50 μm). A blue light-emitting diode was used for fluorescence excitation. The μAPD was operated in Geiger mode to detect the fluorescence. The detection limit of the prototype (~25 nM) was determined by finding the minimum detectable concentration of a solution of fluorescein. The device was used to detect the separation of a mixture of proteins and small molecules by capillary electrophoresis; the separation illustrated the suitability of this integrated fluorescence detection system for bioanalytical applications.

We describe the development of a prototype microfluidic device fabricated in poly(dimethylsiloxane) (PDMS) with an integrated optical detection system and demonstrate the performance of the device by the analysis of proteins and small molecules. Microfluidic systems provide a platform for the rapid analysis and manipulation of biological samples.[1−5] Two potential advantages of microfabricated devices are portability—a reflection of their small sizes—and disposability—a reflection of the low cost that would result from fabrication in large numbers. Although fluidic systems based on microchannels can be very small, optical systems for the detection of biological analytes in these microchannels are still relatively large;[5] the entire system, obviously, can be no smaller than its largest component.[6] The realization of the full advantages of microfluidic devices requires schemes for detection that are small, portable, and inexpensive.

Two tasks must be successfully accomplished to demonstrate a useful detection system for bioanalysis on the microscale: (i) the design and fabrication of components that are suitable for on-chip detection and (ii) the evaluation and optimization of the detector for biochemical analyses. The detection of low concentrations of analytes in the small volumes (nL) of samples present in microfluidic devices requires sensitive analytical techniques. Many schemes—e.g., refractive index,[7] absorption,[8] fluorescence,[8−10] and electrochemical[11−14] —have been explored for the detection of biomolecules in microfluidic devices. Of these techniques, fluorescence detection is generally the most sensitive.[15] Because of

† Harvard University.

‡ Radiation Monitoring Devices, Inc.

(1) Harrison, D. J.; Fluri, K.; Seiler, K.; Fan, Z.; Effenhauser, C. S.; Manz, A. *Science* **1993**, *261*, 895−897.
(2) Ramsey, J. M.; Jacobsen, S. C.; Knapp, M. R. *Nat. Med.* **1995**, *1*, 1093−1096.
(3) Kopp, M. U.; Crabtree, H. J.; Manz, A. *Curr. Opin. Chem. Biol.* **1997**, *1*, 410−419.
(4) Colyer, C. L.; Tang, T.; Chiem, N.; Harrison, D. J. *Electrophoresis* **1997**, *18*, 1733−41.
(5) Kovacs, G. T. A. *Micromachined Transducers Sourcebook*; McGraw-Hill: New York, 1998.
(6) Some electrical components for high-voltage applications are also difficult to minaturize.
(7) Burggraf, N.; Krattiger, B.; de Mello, A. J.; de Rooij, N. F.; Manz, A. *Analyst* **1998**, *123*, 1443−1447.
(8) Liang, Z.; Chiem, N.; Ocvirk, G.; Tang, T.; Fluri, K.; Harrison, D. J. *Anal. Chem.* **1996**, *68*, 1040−1046.
(9) Jiang, G. F.; Attiya, S.; Ocvirk, G.; Lee, W. E.; Harrison, D. J. *Biosens. Bioelectron.* **2000**, *14*, 861−869.
(10) Wang, S.-C.; Morris, M. D. *Anal. Chem.* **2000**, *72*, 1448−1452.
(11) Woolley, A. T.; Lao, K.; Glazer, A. N.; Mathies, R. A. *Anal. Chem.* **1998**, *70*, 684−688.
(12) Rossier, J. S.; Roberts, M. A.; Ferrigno, R.; Girault, H. H. *Anal. Chem.* **1999**, *71*, 4294−4299.
(13) Martin, R. S.; Gawron, A. J.; Lunte, S. M.; Henry, C. S. *Anal. Chem.* **2000**, *72*, 3196−3202.
(14) Zhao, H.; Dadoo, R.; Reay, R. J.; Kovacs, G. T. A.; Zare, R. N. *J. Chromatogr., A* **1998**, *813*, 205−208.
(15) Cruz, L.; Shippy, S. A.; Sweedler, J. V. In *High Performance Capillary Electrohoresis*; Khaledi, M. G., Ed.; John Wiley & Sons: New York, 1998; Vol. 146, pp 303−348.

10.1021/ac010423z CCC: $20.00
Published on Web 08/15/2001

its high sensitivity and widespread use in conventional analytical devices, the majority of work in microfluidic devices has used fluorescence detection, usually implemented using laser-induced fluorescence (LIF) and confocal microscopy.[9,16-18] Although the sensitivities of LIF schemes are excellent (i.e., sufficient to detect single molecules of fluorescent dyes[19]) the size of the associated optics and detector is large relative to the size of the microfluidic chip. The ability to integrate optical components into microfluidic chips is a major challenge in the development of microanalytical systems.

One of the most important components in an optical detection system is the photodetector. The major classes of photodetectors include photodiodes (PDs), charge-coupled devices (CCDs), photomultiplier tubes (PMTs), and avalanche photodiodes (APDs).[20,21] Real-time detector response is an important feature for a number of bioanalytical tasks, such as capillary electrophoresis (CE) [22,23] and cell sorting.[24] CCDs require integration of the photosignal to provide the time necessary to read out data from each individual pixel, and PDs require integration of the photosignal to improve their sensitivity. In contrast, PMTs and APDs are capable of real-time, single-photon response, i.e., photon counting. PMTs are in wide use because they amplify optical signals efficiently and are a well-developed technology.[20] High-gain solid-state detectors, such as APDs, may prove superior to PMTs in applications where low photon fluxes and high sensitivities are required.[25,26] APDs are advantageous because (i) they have a higher quantum efficiency (>50%) than PMTs (10%),[26-29] (ii) they operate at relatively low voltages (40−100V) compared to PMTs (>500 V), and (iii) they should be relatively inexpensive if fabricated in large batches.[30] In addition to their sensitivity, the dimensions of newly available micro-APDs (μAPDs)[29,31] match the dimensions of microfluidic channels (50−100 μm). This feature eliminates the need for transfer optics if the distance that separates the μAPD and the microchannel is small (200 μm). These attributes make μAPDs an obvious target for integration into microfluidic systems.

Polymers are attractive materials for the fabrication of microfluidic systems because they are less expensive and less fragile than glass and silicon, two of the most common materials for microanalytical systems.[18,23,32-41] The optical and chemical properties of PDMS are particularly attractive for the fabrication of a microfluidic system with an integrated optical detection system.[42] PDMS is optically transparent from 235 nm to the near-infrared. This transparency allows for optical detection over the entire visible spectrum. The autofluorescence of PDMS is also lower than that for many polymers such as polystyrene.[10]

Our group and others have developed a comprehensive set of techniques for the rapid prototyping of "microdevices" using PDMS.[23,43-45] The range of devices fabricated in PDMS include microfluidic systems,[18,36,38,39,46,47] microelectromechanical systems,[40,48] and microtransfer optics.[49,50] Features of the rapid-prototyping procedure for PDMS-based devices that are especially important for the fabrication of microanalytical systems include the ability to fabricate 3-D microfluidic systems,[51] the ability to create interconnects with external components,[18,39] and the ability to control the surface chemistry of PDMS.[52]

There are relatively few published examples of the integration of optical components for fluorescence detection into microfluidic devices.[8,53,54] Webster et al. described a monolithic system consisting of a microfabricated silicon photodiode and a Parylene-based microfluidic system.[54] An advantage of their fabrication method is the ability to fabricate optical interference filters using chemical vapor deposition. The main disadvantage of this system is the low

(16) Seiler, K.; Harrison, D. J.; Manz, A. *Anal. Chem.* **1993**, *65*, 1481−1488.
(17) Hadd, A. G.; Raymond, D. E.; Halliwell, J. W.; Jacobson, S. C.; Ramsey, J. M. *Anal. Chem.* **1997**, *69*, 3407−3412.
(18) Duffy, D. C.; McDonald, J. C.; Schueller, O. J. A.; Whitesides, G. M. *Anal. Chem.* **1998**, *70*, 4974−4984.
(19) Goodwin, P. M.; Ambrose, W. P.; Keller, R. A. *Acc. Chem. Res.* **1996**, *29*, 607−613.
(20) Dereniak, E. L.; Crowe, D. G. *Optical Radiation Detectors*; Wiley: New York, 1984.
(21) Voss, K. J. *Methods Enzymol.* **2000**, *305*, 53−62.
(22) Khaledi, M. G. *High Performance Capillary Electrophoresis*; John Wiley Sons: New York, 1998.
(23) McDonald, J. C.; Duffy, D. C.; Anderson, J. R.; Chiu, D. T.; Wu, H.; Schueller, O. J. A.; Whitesides, G. M. *Electrophoresis* **2000**, *21*, 27−40.
(24) Fu, A. Y.; Spence, C.; Scherer, A.; Arnold, F. H.; Quake, S. R. *Nat. Biotechnol.* **1999**, *17*, 1109−1111.
(25) Barber, S. *Electr. Eng.* **1984**, *56*, 63−69.
(26) Dautet, H.; Deschamps, P.; Dion, B.; MacGregor, A. D.; MacSween, D.; McIntyre, R. J.; Trottier, C.; Webb, P. P. *Appl. Opt.* **1993**, *32*, 3894−3900.
(27) Brown, R. G. W.; Jones, R.; Rarity, J. G.; Ridley, K. D. *Appl. Opt.* **1987**, *26*, 2383−2389.
(28) Brown, R. G. W.; Ridley, K. D.; Rarity, J. G. *Appl. Opt.* **1986**, *25*, 4122−4126.
(29) Vasile, S.; Gothoskar, P.; Farrell, R.; Sdrulla, D. *IEEE Trans. Nucl. Sci.* **1997**, *45*, 720−723.
(30) In principle, if APDs are fabricated in large enough quantities, they could be considered for use in disposable devices.
(31) Vasile, S.; Wilson, R. J.; Shera, S.; Shamo, D.; Squillante, M. R. *IEEE Trans. Nucl. Sci.* **1999**, *46*, 848−852.
(32) Schützner, W.; Kenndler, E. *Anal. Chem.* **1992**, *64*, 1991−1995.
(33) Bayer, H.; Engelhardt, H. *J. Microcolumn Sep.* **1996**, *8*, 479−484.
(34) Roberts, M. A.; Rossier, J. S.; Bercier, P.; Girault, H. *Anal. Chem.* **1997**, *69*, 2035−2042.
(35) Martynova, L.; Lacascio, L. E.; Gaitan, M.; Kramer, G. W.; Christensen, R. G.; MacCrehan, W. A. *Anal. Chem.* **1997**, *69*, 4783−4789.
(36) Effenhauser, C. S.; Bruin, G. J. M.; Paulus, A.; Ehrat, M. *Anal. Chem.* **1997**, *69*, 3451−3457.
(37) DeBusschere, B. D.; Borkholder, D. A.; Kovacs, G. T. A. *Solid-State Sensor and Actuator Workshop;* Hilton Head Island, SC, June 1998; pp 358−362.
(38) Ocvirk, G.; Munroe, M.; Tang, T.; Oleschuk, R.; Westra, K.; Harrison, D. J. *Electrophoresis* **2000**, *21*, 107−115.
(39) Unger, M. A.; Chou, H.-P.; Thorsen, T.; Scherer, A.; Quake, S. R. *Science* **2000**, *288*, 113−116.
(40) Soper, S. A.; Ford, S. M.; Qi, S.; McCarley, R. L.; Kelly, K.; Murphy, M. C. *Anal. Chem.* **2000**, *72*, 643A−651A.
(41) Beebe, D. J.; Moore, J. S.; Yu, Q.; Liu, R. H.; Kraft, M. L.; Jo, B.-H.; Devadoss, C. *Proc. Natl. Acad. Sci. U.S.A.* **2000**, *97*, 13488−13493.
(42) Dow Corning Corp., Midland, MI.
(43) Xia, Y.; Whitesides, G. M. *Angew. Chem., Int. Ed.* **1998**, *37*, 550−575.
(44) Jo, B.-H.; Van Lerberghe, L. M.; Motsegood, K. M.; Beebe, D. J. *J. Microelectromech. Syst.* **2000**, *9*, 76−81.
(45) Quake, S. R.; Scherer, A. *Science* **2000**, *290*, 1536−1540.
(46) Folch, A.; Ayon, A.; Hurtado, O.; Schmidt, M. A.; Toner, M. *J. Biomech. Eng.* **1999**, *121*, 28−34.
(47) Chou, H.-P.; Spence, C.; Schere, A.; Quake, S. *Proc. Natl. Acad. Sci. U.S.A.* **1999**, *96*, 11−13.
(48) Schueller, O. J. A.; Brittain, S. T.; Marzolin, C.; Whitesides, G. M. *Chem. Mater.* **1997**, *9*, 1399−1406.
(49) Wilbur, J. L.; Jackman, R. J.; Whitesides, G. M.; Cheng, E.; Lee, L.; Prentiss, M. *Chem. Mater.* **1996**, *8*, 1380−1385.
(50) Zhao, X.-M.; Stoddart, A.; Smith, S. P.; Kim, E.; Xia, Y.; Prentiss, M.; Whitesides, G. M. *Adv. Mater.* **1996**, *8*, 420−424.
(51) Anderson, J. R.; Chiu, D. T.; Jackman, R. J.; Cherniavskaya, O.; McDonald, J. C.; Wu, H.; Whitesides, S. H.; Whitesides, G. M. *Anal. Chem.* **2000**, *72*, 3158−3164.
(52) Chaudhury, M. K.; Whitesides, G. M. *Science* **1991**, *255*, 1230−1232.
(53) Hubner, J.; Mogensen, K. B.; Jorgensen, A. M.; Friis, P.; Telleman, P.; Kutter, J. P. *Rev. Sci. Instrum.* **2001**, *72*, 229−233.
(54) Webster, J. R.; Burns, M. A.; Burke, D. T.; Mastrangelo, C. H. *Anal. Chem.* **2001**, *73*, 1622−1626.

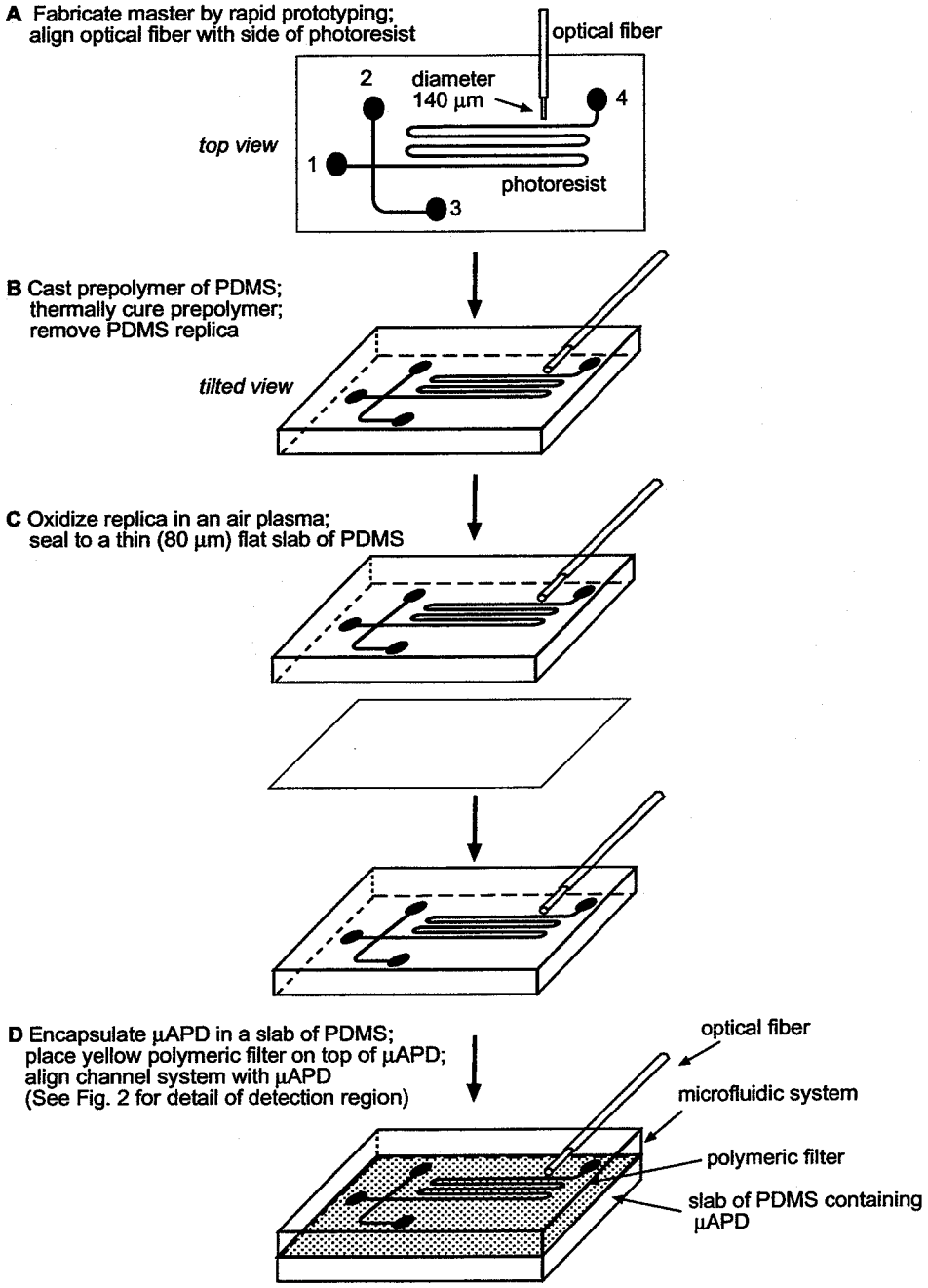

Figure 1. Scheme that shows the procedure used for fabricating an integrated fluorescence detection system in PDMS. The features in the figure are not to scale. (A) A 100-μm core diameter fiber was aligned perpendicularly to the relief pattern of photoresist on a silicon wafer. The relief of photoresist forms the microchannels upon replica molding. (B) PDMS prepolymer was poured onto the master and the aligned optical fiber and cured. (C) Once cured, the PDMS replica with the molded optical fiber was removed from the support and sealed to a thin (80 μm) membrane of PDMS. A polymeric yellow filter (Roscolux No. 312 canary yellow) was conformally sealed to the bottom (the thin membrane) of the sealed device. (D) The device was aligned and placed onto the active area of a μAPD embedded in PDMS.

quantum efficiency of the photodiode below 550 nm, a region where many widely used fluorescent markers emit light. Hubner et al. reported the fabrication of a microfluidic device and integrated waveguides in silica using chemical vapor deposition.[53] The silica waveguides were used to deliver the excitation light and collect the fluorescence. Harrison et al. reported a microfluidic system fabricated in glass where optical fibers were inserted in channels in the device and used for detection of both absorbance and fluorescence.[8] All of these methods utilize conventional techniques for microfabrication that can limit the ability to test new designs rapidly.

This paper describes an integrated fluorescence detection system using a μAPD and a microfluidic system fabricated in PDMS. Our system consisted of the following components: (i) an optical fiber, oriented perpendicularly to a microfluidic channel, to couple excitation light from a blue LED into the microchannel, (ii) polymeric colored filters to prevent scattered excitation light from reaching the detector, and (iii) a μAPD, placed adjacent to the microchannel and perpendicular to the optical fiber, to detect fluorescent analytes. To demonstrate the utility of this optical detection system, we have examined a separation and detection of a mixture of proteins and small molecules by CE.

RESULTS AND DISCUSSION

Fabrication of the Device. *Integration of the Optical Fiber into the Microfluidic System.* To fabricate devices in PDMS, we used a procedure for rapid prototyping that has been described in detail elsewhere.[18] We briefly outline the method here, focusing on details relevant to the integration of fiber optics (Figure 1). First, we used standard photolithography to fabricate a master for the microfluidic channels consisting of a positive relief of photoresist on a Si wafer. Next, a multimode silica optical fiber (100-μm core diameter, 140-μm total diameter with cladding), which had been stripped of its protective polymeric coating, was placed approximately 50−100 μm away from the photoresist on the wafer and near the end of the separation channel.[55] The optical fiber was clamped in place using a simple mounting stage, PDMS prepolymer was poured over the master and optical fiber, and the ensemble was cured in an oven at 70 °C for 1 h. This procedure did not adversely affect the performance of the optical fiber. The channel system was removed from the master, and reservoirs were fabricated using a circular metal punch. We sealed the channel system irreversibly to a thin (~80 μm) flat piece of PDMS using a procedure based on plasma oxidation of PDMS.[18,56] Immediately after sealing the fluidic system, we filled the channel with aqueous buffer to preserve the hydrophilic layer on the channel walls that resulted from the plasma oxidation.[18,57] An 80-μm-thick, yellow polycarbonate filter was then conformally sealed to the bottom (the thin PDMS film) of the channel system.

The method of fabrication described here is similar to that used by Harrison to integrate optical fibers with microfluidic systems[8] but differs in several regards: (i) the procedure used for fabrication is simpler than the procedure of Harrison because it is based on an efficient method for prototyping; (ii) the PDMS conforms to the surface of the optical fiber; this molecular-level contact obviates the need for index matching liquid that is required for optical fibers that are inserted into channels; and (iii) we used a multimode optical fiber with a core diameter that was similar to the size of the microchannel; the similar size eased the alignment of the two. The method developed by Harrison has the advantage that the position of the fiber relative to the microfluidic channel is precisely defined by the microchannel into which the fiber is inserted. In our devices, the exact distance between the tip of the optical fiber and the microchannel was not critical because of the low divergence angle of the light that was emitted from the fiber (vide infra).

Embedding the μAPD in PDMS. Radiation Monitoring Devices, Inc. (RMD) provided a prototype array of Geiger-mode μAPDs.[58] μAPDs have high quantum efficiency and are able to detect single-photon events. Various aspects of the fabrication and performance characteristics of the μAPDs are described in the literature.[29,31] The prototype μAPDs were fabricated in a planar array of 117 individual elements, or pixels, in various sizes.[59] The individual

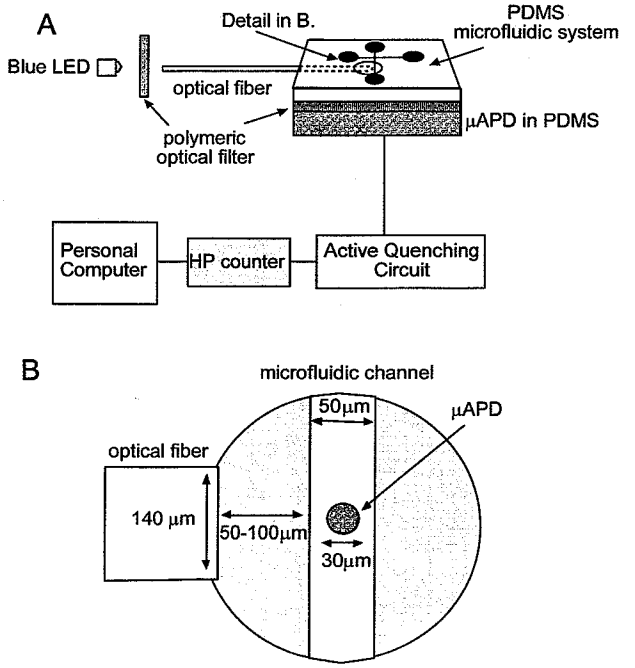

Figure 2. Diagrams of the experimental setup used and the arrangement of the μAPD with respect to the optical fiber and channel. (A) The light from a blue LED was coupled into the optical fiber to excite fluorophores in the channel. The isotropically emitted photons were detected by the actively quenched μAPD. The photocounts from the quenching circuit were counted with an HP universal counter interfaced with a personal computer. (B) The detail of the excitation/detection region.

pixel elements were connected to the external active-quenching and detection circuitry by wire bonds. We conducted all experiments with 30-μm-diameter pixels because their size was commensurate with the width of microfluidic channels used for CE.

We designed a system that allowed us to reuse the μAPD array because the μAPDs were research prototypes and were fabricated in limited numbers. This configuration represents a potential portable device where the detection system is reusable, but the microfluidic system is disposed of after the analysis of a sample. The μAPD array was embedded in PDMS by placing the array face down on a silanized silicon wafer and then pouring PDMS prepolymer around it; light pressure (~10 g/cm^2) was applied to the array to press it against the wafer. This procedure allowed PDMS to wick under the wire-bonded array and to create a thin (<50 μm) membrane over the surface of the μAPD array. The PDMS was cured at room temperature over several days, rather than at 70 °C, to avoid the possibility of mechanical stress on the wire bonds to the μAPDs. The PDMS membrane over the μAPD array was fragile because the PDMS did not adhere well to the array; however, it was sturdy enough to withstand careful manipulation. The embedding process did not affect the performance of the μAPDs.

The device was designed so that the fluidic system could be reversibly sealed to the μAPD array embedded in PDMS. The two components were aligned and assembled by hand under a stereoscope at 50× magnification. The fluidic system and μAPD array were aligned such that the area of the microchannel near the optical fiber was placed over an individual μAPD (Figure 2). We verified that the optical fiber and μAPD were properly

(55) The spacing between the optical fiber and photoresist was necessary because distortions of the microchannel occurred if the fiber was in contact with the photoresist during the curing process of the PDMS.
(56) Chaudhury, M. K.; Whitesides, G. M. *Langmuir* **1991**, *7*, 1013−1025.
(57) Morra, M.; Occhiello, E.; Marola, R.; Garbassi, F.; Humphrey, P.; Johnson, D. *J. Colloid Interface Sci.* **1990**, *137*, 11−24.
(58) Although these μAPDs are not yet commercially available, they are commerical prototypes.
(59) We did not exploit the use of multiple pixels in these experiments; only one pixel was used at a time.

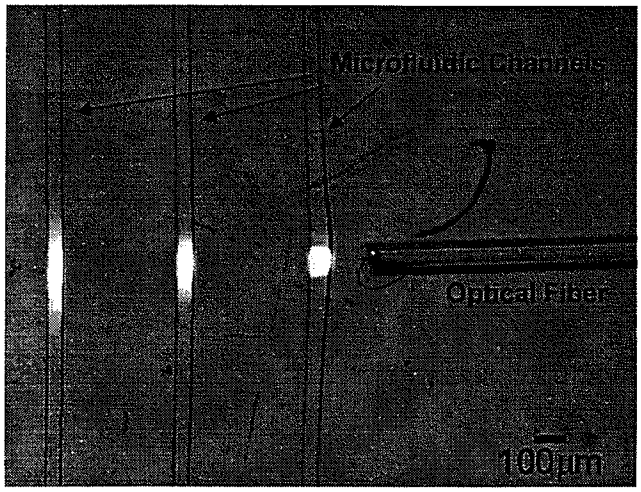

Figure 3. Fluorescence micrograph showing the size of the probe volume. The channel was filled with 1 mM fluorescein, and fluorescence was excited by light coupled into the fiber optic from the blue LED. The excitation light diverged after leaving the tip of the fiber. This divergence is evident as the volume of excitation becomes progressively larger, and the fluorescence grows more diffuse in the channels that are farther away from the fiber. The measured angle of divergence of the beam (~12°) is in agreement with the NA (0.29) of the fiber. The probe volume of 0.25 nL is defined by the dimensions of the channel (50 μm wide and 50 μm deep) and by the width of the excitation beam (~100 μm). The slight bulge in the microchannel closest to the optical fiber is due to a distortion in the PDMS caused by the optical fiber during the curing process. This bulge did not affect the performance of the device.

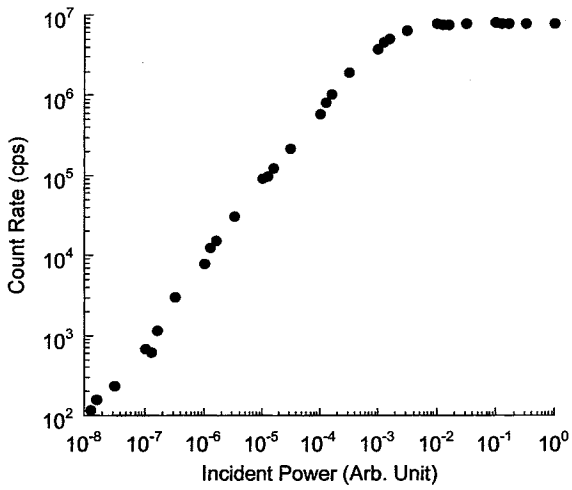

Figure 4. Dependence of the photon count rate of the actively quenched, Gieger mode, μAPD device (41 V bias) on the power of the incident light. The dark count rate has been subtracted. The small deviations in linearity are attributed to systematic errors introduced by the stacking of multiple reflective optical density filters used to reduce the power of the incident light.

aligned by measuring the Geiger mode signal from the μAPD when light was sent through the optical fiber.

Optical Components and Performance of the Detector. *Coupling of Excitation Light from the Light-Emitting Diode (LED) into the Optical Fiber.* A blue LED was chosen as the excitation source. A number of other groups have recently used blue LEDs for fluorescence excitation in microfluidic devices.[10,54,60] The LED emits a broad band of light with a fwhm of ~25 nm that is centered at 473 nm. This peak was near the absorption maximum of fluorescein at 490 nm. We coupled the light into the fiber by positioning the free tip of the optical fiber near the LED using a simple optical positioner (Figure 2). The alignment was optimized by measuring the signal detected by the μAPD and repositioning the fiber relative to the LED. After optimization, a blue polymeric film was placed between the fiber and LED to filter the excitation light. The filter reduced the intensity of the excitation light at wavelengths that were shorter than the excitation maximum of fluorescein.

Size of the Excitation Volume. The excitation volume (~0.25 nL) was defined by the width of the optical fiber and the cross-sectional area of the channel (Figure 3). The blue light from the fiber diverges over several hundred micrometers to a width defined by the numerical aperture (NA) of the fiber (0.29).[61] These data demonstrate two important features of the optical system. First, the conformal contact between the PDMS and the optical fiber eliminates index matching problems that can occur when optical fibers are inserted in micromachined channels. Second, the channel in the microfluidic device has a flat wall that reduces the optical distortions typically observed in cylindrical capillaries.[62] The width of the region illuminated by the light from the fiber (~100 μm) was small relative to the width of a typical peak in an electrophoretic separation (1–10 mm). The tip of the fiber, therefore, did not need to be immediately adjacent to the channel.

Performance of the mAPD. We used the μAPD in Geiger mode to count the fluorescence photons in our experiments. In Geiger mode operation, the μAPD is biased above the breakdown point; when a photon strikes the surface of the μAPD, an electron cascade (an avalanche) is created in the region of high electric field in the device leading to a large gain in current. The performance of the μAPD in Geiger mode depends strongly on the bias voltage and its dead time.[25,26,29] In our prototype, the μAPD was connected to a proprietary active quenching circuit built by RMD that exhibited a dead time of ~50 ns and a dynamic range suitable for the experiments that we conducted. At a bias voltage of 41 V, we generally observed 600 ± 50 dark counts/s at room temperature using the active quenching circuit. This value varied from pixel to pixel because of minor nonuniformities in the μAPDs. This rate sets the lower limit of the sensitivity to ~32 counts/s based on a simple estimate of the shot noise of the device. The maximum count rate possible with our quenching circuit was ~10^6 counts/s (Figure 4).

Detection of Fluorescence. The fluorescence from analytes in the microfluidic system was detected by photon counting with the μAPD. The photon counts were collected over a 500-ms interval. Prior to each run, we filled the microfluidic system with buffer and measured the background count rate with the excitation light off and with the excitation light on.

The collection efficiency of the fluorescence photons by the μAPD should decrease as the square of the distance from the channel as the solid cone angle that intersects the pixel decreases.

(60) Malik, A. K.; Fauberl, W. *Chem. Soc. Rev.* **2000**, *29*, 275–282.

(61) The numerical aperature, NA, of the fiber defines the angle of light that can be launched into (or emitted from) the fiber. NA = ns in(α) where n is the refractive index of the medium of propagation and α is the angle of dispersion from the center point of the fiber (See Figure 3.).

(62) Tsuda, T.; Sweedler, J. V.; Zare, R. N. *Anal. Chem.* **1990**, *62*, 2149–2152.

We estimate that the channel system was 200 μm from the μAPD based on the sum of the thicknesses of the PDMS film sealed to the microchannel, the polymeric filter, and the membrane of PDMS over the μAPD. If we consider a point source in the bottom center of the channel, the solid cone angle captured by the μAPD is ~8°. This leads to an estimated collection efficiency of 0.2%; this value represents the fraction of the surface area of a sphere centered at the point source that intersects the surface area of the μAPD. This efficiency is low compared to that obtained by techniques that use transfer optics; e.g., for an oil immersion objective with a NA of 1.4, the collection efficiency could be as high as 25%. We believe that we can improve the collection efficiency by decreasing the distance between the μAPD and microchannel by using a thinner polymeric filter or by using the PDMS film that forms the floor of the channel as a filter by doping it with an appropriate dye. The use of an external reflecting mirror on the surface of the channel system could also increase the collection efficiency, but we did not explore these options in the prototype described here.

A polymeric optical filter was used to isolate the fluorescence signal from the excitation light.[63] We used proteins that were labeled with fluorescein in our CE experiments. Fluorescein has an absorption maximum at 494 nm, a value well matched to the output spectrum of the LED, and an emission maximum at 520 nm. The filters were chosen to transmit as much of the fluorescence as possible, while blocking as much of the excitation light as possible.[64] The background photon count rate that we measured while the LED illuminated the channel with the filters in place was typically a factor of 5 higher than the dark count rate. This background count rate varied by as much as a factor of 2 from device to device and depended on the position of the optical fiber relative to the μAPD. Any increase in collection efficiency will also increase this background signal. We therefore believe that the optical filtering of the excitation light is the most critical factor that limits our sensitivity. Although this background ultimately limits the sensitivity of our prototype, it does not affect the validation of the technique.

Sensitivity of the Integrated Fluorescence Detection System. The sensitivity of our integrated device was established by filling the microchannel with solutions containing known concentrations of fluorescein. We filled the fluidic channel with solutions containing progressively higher concentrations of fluorescein using pressure-driven flow and measured the count rate of the μAPD (Figure 5). The channel was then flushed with buffer, and the process was repeated. The minimum concentration detected was ~25 nM; the count rate observed at this concentration was ~1000 counts/s higher than the signal obtained with buffer in the channel. This count rate is well above the noise level of the device and is a conservative detection limit. The minimum detectable concentration was reproducible to within 10 nM for three separate devices.[65] At ~25 μM, the count rate reached the saturation point of our prototype device. These limits defined the linear response range of our device to be ~3 orders of magnitude.[66] These limits were adequate for the sample concentrations, 0.1–1.0 μM, typically used in analytical separations such as CE.[15]

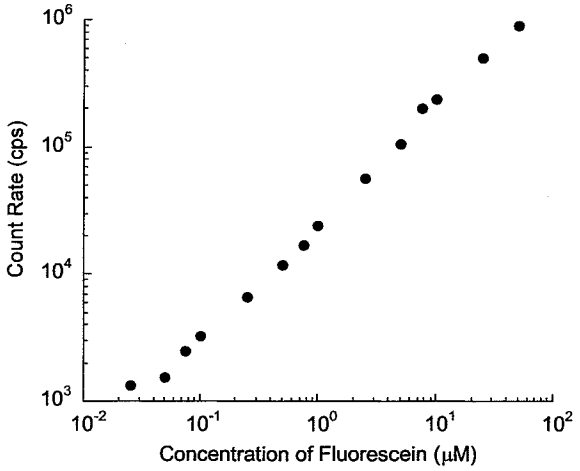

Figure 5. Detected photon count rate as a function of fluorescein concentration in a sodium borate buffer solution (pH 9.2). The background signal in the presence of buffer was 600 ± 50 counts/s with the LED turned off and 3000 ± 300 counts/s with the LED turned on.

Capillary Electrophoresis. To demonstrate the capabilities of a device that coupled separation and detection, we performed a separation using CE in the prototype system.[1,4,22] Since the separation of proteins is an important application of microfluidic devices,[3,4,67–69] we chose to separate a mixture of proteins and small molecules to test the device. We covalently labeled two proteins (carbonic anhydrase and α-lactalbumin) with ~1 equiv of fluorescein. This labeling procedure ensured that the fluorescence signal was not self-quenched by the presence of multiple fluorescein molecules and that the detected signal was directly proportional to the concentration of protein.

We performed the separation using a procedure that we have previously described.[18] In brief, we accomplished the injection using electrokinetic pumping and the separation of the sample using capillary zone electrophoresis in the microfluidic device. The voltages were controlled using a LabView program that also acquired the signal from the quenching circuit of the μAPD. Despite the proximity of the high-voltage electrodes and the presence of high electric fields in the electrophoresis channel (0.1 MV/m), we did not observe any significant electrical interference from the high-voltage source at the photodetector. PDMS is an excellent electrical insulator and prevented arcing between the high-voltage electrodes and the μAPD.[42]

Figure 6A shows the electropherogram obtained using the integrated device. All four compounds were resolved with baseline resolution. The count rate at the apex of the most intense peak

(63) We did not observe a fluorescence signal from the polymeric colored filters using fluorescence microscopy with a mercury lamp for excitation.

(64) The output spectrum of the blue LED and the absorbance spectra of the polymeric filters are included in the Supporting Information.

(65) While the detection limit for a given prototype might be lower than 25 nM, we prefer this conservative limit because of the variability in optical geometry from the rapid-prototyping method. This limit is more than adequate for the validation of the prototype for bioanalysis.

(66) For comparison, a Beckman CE (P/ACE model) is able to detect concentrations of fluorescein of 10 pM with a dynamic range of $>10^4$ using laser-induced fluorescence. Beckman-Coulter (Fullerton, CA).

(67) Haynes, P. A.; Gygi, S. P.; Figeys, D.; Aebersold, R. *Electrophoresis* **1998**, *19*, 1862–1871.

(68) Collins, F. S.; Patrinos, A.; Jordan, E.; Chakravarti, A.; Gesteland, R.; Walters, L. *Science* **1998**, *282*, 682–689.

(69) Fields, S. *Science* **2001**, *291*, 1221–1224.

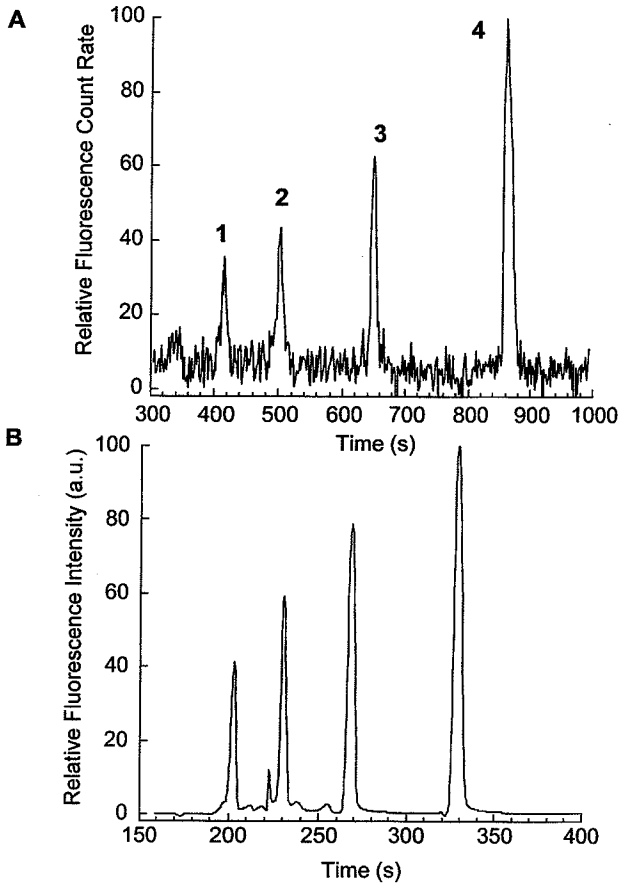

Figure 6. Electropherograms of a ~5 μM mixture of (1) fluorescein-labeled carbonic anhydrase, (2) fluorescein-labeled α-lactalbumin, (3) fluorescein, and (4) 5-carboxyfluorescein in 25 mM Tris/182 mM Gly/100 mg/mL QPS. (A) Separation in the prototype microfluidic device. The length of the separation channel was 24.3 cm, and the distance from injection to detection was 18.8 cm. The separation voltage was 3150 V. (B) Separation in a Beckman P/ACE using LIF detection. The length of the fused-silica capillary was 27 cm, and the distance from injection to detection was 20 cm. The separation voltage was 5000 V.

was ~1500 counts/s higher than the background. This value corresponds to ~50 nM fluorescein based on our sensitivity data (Figure 5) and is consistent with a dilution factor of ~100 from our sample concentration (5 μM) during the separation. This estimate of the dilution factor is reasonable based on the dispersion of the sample plug during the separation. Figure 6B shows the electropherogram for the same sample obtained from a commercial CE system using LIF excitation and a PMT as the photodetector. The resolution of the chromatographic peaks was identical to that from the prototype device. The performance of the prototype system was comparable to the commercial instrument even though our detection limit (25 nM) was ~1000 times higher than that of the commercial instrument (10 pM). The higher performance of the commercial instrument is primarily due to its optical filtering, which cleanly isolates the fluorescence signal from the excitation light. Other factors, such as optimized circuitry, reflective mirrors for light collection, and the higher excitation power available from the laser also contribute to the improved performance of the commercial system. The device based on the μAPD thus has a lower sensitivity than the commercial instrument, but also has a lower cost, smaller size, and simpler design.

CONCLUSIONS

We have described the integration of a fluorescence detector based on a μAPD into a microfluidic device fabricated in PDMS. This design provides the basis for a platform for a portable (and perhaps, disposable) microfluidic system incorporating a μAPD because the data acquisition hardware could, in principle, be miniaturized. The benefits of this device include the following assets: (i) The design of the system allows for a disposable fluidic system with a reusable detection system. (ii) All the components are readily available, except for the prototype μAPD, and are inexpensive. (iii) Our fabrication technique of embedding the optical fiber in PDMS eliminates the problems of index matching that have proved troublesome in micromachined devices. (iv) The diameter of the μAPDs is comparable to the width of microfluidic channels; this matching in size eliminates the need for collection optics.

The μAPD used in this work is an engineering prototype, and the information summarized in this paper demonstrates the level of performance that can be obtained without exhaustive optimization. There are a number of routes to improve the performance of the device. The first and most important would involve the use of better filters to isolate the fluorescence from the excitation light. Other useful improvements that could be made include the following: (i) The pixel size of the μAPD could be increased to the width of the channel to increase the number of photons collected. (ii) The distance between the channel and the μAPD could be decreased to improve the collection efficiency. (iii) An external reflecting mirror could be added to the upper surface of the channel above the μAPD to increase the number of collected photons.

We have focused on the integration of a single pixel from an array of μAPDs for use as a point source detector. The ability to integrate an array of μAPDs for parallel monitoring of multiple sites in a microfluidic system will be valuable in applications that involve parallel analyses and high-throughput screening.[69,70] The integrated detection system described here represents a step toward fully integrated, sensitive, portable, and economical microfluidic devices.

EXPERIMENTAL SECTION

Fabrication. *Rapid Prototyping.* Designs of networks of microfluidic channels (diameters >20 μm) were created in a CAD program (Freehand 8.0, Macromedia, San Francisco, CA). Transparencies with high-resolution features were produced (Herkules PRO image setter, 5080 dpi, Linoytype-Hell Co., Hauppauge, NY) from the CAD files with the design clear and the background ink. Transparencies were used as masks in photolithography on negative photoresist (SU-850, Micro. Chem. Corp., Newton, MA) spin-coated onto silicon wafers to create masters. We spin-coated at 3000 rpm for 20 s to create a layer of photoresist that was 50 μm thick. This thickness defined the height of the features created by photolithography and hence the channels. After development in propylene glycol methyl ether acetate (Sigma-Aldrich, Milwaukee, WI), the masters were placed in a desiccator under vacuum for 2 h with a vial containing a few drops of tridecafluoro-1,1,2,2-tetrahydrooctyl-1-trichlorosilane (United Chemical Technologies, Bristol, PA): silanization of the master facilitates the removal of the PDMS replica after molding.

(70) Bernard, A.; Michel, B.; Delamarche, E. *Anal. Chem.* **2001**, *73*, 8–12.

Molding. A 10:1 mixture of PDMS prepolymer and curing agent (Sylgard 184, Dow Corning, Midland, MI) was stirred thoroughly and then degassed under vacuum. The prepolymer mixture was poured onto the master and cured for 1.5 h at 70 °C. After curing, the PDMS replica was peeled from the master. Fluid reservoirs were fabricated by drilling holes in the replica with a circular punch. Flat pieces of PDMS were formed by spin coating the prepolymer on a silanized silicon wafer at 1000 rpm for 30 s and curing.

Sealing. Dust was removed from a PDMS replica and a flat piece of PDMS using Scotch brand transparent tape. The two pieces of PDMS were placed in a plasma cleaner (PDC-32G, Harrick) and oxidized for 1 min. The plasma was generated from room air at ambient humidity at 1.5–2 Torr and 100 W of radio frequency power. Within 30 s after removal from the plasma cleaner, the surfaces were brought into conformal contact, and an irreversible seal formed spontaneously. The polymeric filter was conformally sealed to the bottom of the fluidic system by simple mechanical contact.

Optical Components. The optical fiber (F-MLD-T) was obtained from Newport Corp. (Newport, RI). The fiber had a 100-μm core diameter, a 140-μm cladding diameter, and a polyimide protective coating. The polyimide coating was removed from ~1 cm of the fiber measured from the tip by burning the coating with a match. The removal of the coating ensured that the core of the optical fiber overlapped with as much of the height of the channel as possible. A 6000 millicandela (mcd) luminosity blue LED was purchased from Hosfelt Electronics, Inc (Steubenville, OH).

Microavalanche Photodiode and Detection Electronics. The μAPD was attached to a proprietary active quench circuit that produced a TTL level pulse for each detected photon. The μAPD was biased at 41 V. The photon counts from the active quench detection circuit were acquired using a Hewlett-Packard universal counter (model 5334A) interfaced to a PC via a GP-IB card and a custom LabView program (National Instruments, Austin, TX).

Capillary Electrophoresis. *Preparation of Sample.* Solutions of 200 mM bovine carbonic anhydrase II and 200 mM α-lactalbumin (Sigma) were prepared in deionized water. Aliquots of 200 μL of these solutions were mixed first with 1 μL of 0.1 M NaOH and then with 5 μL of 5 mM 5-carboxyfluorescein, succinimidyl ester (0.5 equiv, Molecular Probes Eugene, OR) in dimethylformamide. After 30 min, the samples were purified on a NICK spin column (Amersham-Pharmacia). The injection sample was prepared by mixing 50 μL each of labeled carbonic anhydrase, 10 μM fluorescein (Sigma-Aldrich), and 10 μM 5-carboxyfluorescein (Molecular Probes) and 100 μL of labeled α-lactalbumin together. The concentrations of the mixture were chosen to give approximately equal peak heights in the micromolar range. The running buffer was 25 mM Tris/192 mM Gly buffer containing 100 mg/mL 3-quinuclidinopropanesulfonate (QPS).[18]

Injection and Separation. The network of channels for CE have been described previously: a separation channel connected to an injection channel through a double-T geometry.[18,71] Reservoirs for fluids were present at each end of the channels.[18] The channel numbering system used here corresponds to that shown in Figure 1. A solution containing the analytes was placed in reservoir 2. The running buffer, 25 mM Tris/192 mM Gly/100 mg/mL QPS, was placed in the other reservoirs. Applying a potential of 150 V at reservoir 2 and −150 V at reservoir 3 caused an electroosmotic flow (EOF) that pumped the analytes from reservoir 2 through the double-T to reservoir 3. Applying a potential of 120 V at reservoir 1 and 500 V at reservoir 4 prevented the analytes from flowing down the separation channel during injection because of slight mismatches in the heights of the columns of fluid in the reservoirs. Separation of the plug of analytes occurred by applying voltages of 150 V at reservoir 1 and −3000 V at reservoir 4. The analytes then moved toward reservoir 4 at rates determined by the EOF of the channel and their electrophoretic mobilities. A potential of −150 V was applied to reservoirs 2 and 3 to prevent reinjection of the sample during separation. The voltages were generated for reservoir 4 by a commercial kilovolt power supply (reservoir 4, CZE1000R, Spellman, Hauppauge, NY) and for reservoirs 1–3 by a custom-made, multichannel supply based on power op amps (PA42, Apex Microtechnology) and powered by a ±150 V power supply (Lambda). The voltages were controlled using an analog output board (AT-AO-10, National Instruments) and LabView. *Warning: Extreme care should be exercised when using high-voltage power supplies.*

CE in Fused-Silica Capillaries. Electrophoretic separations in a 50-μm-i.d., 365-μm-o.d. fused-silica capillary (Polymicro Technology, Phoenix, AZ) were performed on a PACE 5000 CE instrument (Beckman Instruments, Fullerton, CA) fitted with an LIF source and detector. Samples were pressure injected and separated at 5 kV in the same buffer as used in the separation in the microfluidic system.

ACKNOWLEDGMENT

We thank DARPA (BioFlips Program) and the Army (Contract DAAD13-00-C-5003) for funding this work. We thank Prof. G. T. A. Kovacs (Cepheid Inc. and Stanford University) for providing a prototype high-voltage programmable power supply. M.L.C. thanks the NIH for a postdoctoral fellowship.

SUPPORTING INFORMATION AVAILABLE

Transmission spectra of the polycarbonate filters and the emission spectrum of the blue LED. This material is available free of charge via the Internet at http://pubs.acs.org.

Received for review April 16, 2001. Accepted July 6, 2001.

AC010423Z

(71) Waters, L. C.; Jacobson, S. C.; Kroutchinina, N.; Khandurina, J.; Foote, R. S.; Ramsey, J. M. *Anal. Chem.* **1998**, *70*, 5172–5176.